

Ryk controls remapping of motor cortex during functional recovery after spinal cord injury

Edmund R Hollis II^{1,3}, Nao Ishiko¹, Ting Yu¹, Chin-Chun Lu¹, Ariela Haimovich¹, Kristine Tolentino¹, Alisha Richman¹, Anna Tury¹, Shih-Hsiu Wang^{2,3}, Maysam Pessian¹, Euna Jo¹, Alex Kolodkin² & Yimin Zou¹

Limited functional recovery can be achieved through rehabilitation after incomplete spinal cord injury. Eliminating the function of a repulsive Wnt receptor, *Ryk*, in mice and rats by either conditional knockout in the motor cortex or monoclonal antibody infusion resulted in increased corticospinal axon collateral branches with presynaptic puncta in the spinal cord and enhanced recovery of forelimb reaching and grasping function following a cervical dorsal column lesion. Using optical stimulation, we observed that motor cortical output maps underwent massive changes after injury and that hindlimb cortical areas were recruited to control the forelimb over time. Furthermore, a greater cortical area was dedicated to controlling the forelimb in *Ryk* conditional knockout mice than in controls (wild-type or heterozygotes). In the absence of weekly task-specific training, recruitment of ectopic cortical areas was greatly reduced and there was no significant functional recovery even in *Ryk* conditional knockout mice. Our study provides evidence that maximal circuit reorganization and functional recovery can be achieved by combining molecular manipulation and targeted rehabilitation.

A large proportion of spinal cord injury patients have incomplete lesions, where parts of the spinal cord tissues remain intact. Due to the strong inhibitory environment in the injured adult spinal cord, especially in the glial scar, and reduced growth potential of adult axons, the original connections are usually not restored. Nonetheless, the complex circuitry can undergo remodeling to achieve variable levels of functional recovery with rehabilitative training. The molecular and circuit mechanisms underlying such functional recovery are poorly understood. The study of both circuit plasticity and its molecular control will provide important biological basis for treating paralysis.

Functional restoration of the corticospinal motor system after spinal cord injury is of primary importance since it is essential for recovery of voluntary motor control¹. In rodents, however, the role of the corticospinal tract (CST) is more limited, with little effect on locomotion and hindlimb usage¹. Nevertheless, the CST is crucial for skilled forelimb motor control^{1–3}. Fine motor skills are lost after a dorsal column lesion of the main CST, with a varying extent of spontaneous recovery^{4,5}. Therefore, we used a forelimb reaching and grasping task to study how skilled forelimb function is lost after lesion, how it recovers, and what limits its recovery.

Previous work in our lab has demonstrated that Wnt signaling, which regulates axon guidance in development, has a profound effect on axon plasticity after injury in the adult spinal cord^{6–9}. To specifically test the function of Wnt–*Ryk* signaling in neurons, we generated a conditional allele of *Ryk*, encoding a repulsive Wnt receptor, performed motor-cortex-specific knockout and then lesioned the dorsal columns at cervical spine segment 5 (C5). Following *Ryk* conditional knockout, mice recovered on a skilled forelimb reaching task to $81 \pm 7\%$ of

peak pre-injury levels at 12 weeks after dorsal column lesion, compared to only $60 \pm 5\%$ in wild-type control mice. This additional recovery depends on the segment of the main CST immediately rostral to the lesion (C3–C5), as a second dorsal column lesion at C3 reduces the functional recovery of conditional knockout to control levels. Anatomical analyses showed significantly increased collateral sprouting of CST above and below the C5 injury and with presynaptic puncta in these axon sprouts.

Using an optogenetic approach, we monitored the output map of the motor cortex. We found that, immediately after C5 dorsal column lesion, forelimb elbow flexion can be activated by a much larger cortical area, whereas forelimb extension was lost. Over time, the area that activates forelimb flexion reduced back to the original size and a new area, which used to activate the hind limb, was recruited to activate forelimb extension. After the second lesion at C3, the control of forelimb flexion was lost but this new control of forelimb extension was largely unaffected. In *Ryk* conditional knockout (cKO) mice, these changes are more gradual and persistent, and a greater cortical area controls both the forelimb extension and flexion in cKO. Finally, mice that did not undergo weekly behavioral testing displayed only limited skilled forelimb recovery, with performances similar to those of mice tested at 1 week after injury. In the absence of weekly testing, refinement of cortical motor maps was also impaired, irrespective of *Ryk* conditional deletion, highlighting the importance of targeted plasticity.

We demonstrate here that the cortical motor map undergoes dramatic changes to achieve recovery and this reorganization requires continued task-specific training. We also show genetic evidence demonstrating Wnt signaling as important regulator of axon plasticity in

¹Neurobiology Section, Biological Sciences Division, University of California, San Diego, La Jolla, California, USA. ²Solomon H. Snyder Department of Neuroscience, Howard Hughes Medical Institute, The Johns Hopkins School of Medicine, Baltimore, Maryland, USA. ³Present addresses: Burke Medical Research Institute, White Plains, New York, USA, and Brain and Mind Research Institute at Weill Cornell Medicine, New York, New York, USA (E.R.H.); Department of Pathology and Cell Biology, Columbia University School of Medicine, New York, New York, USA (S.-H.W.). Correspondence should be addressed to Y.Z. (yzou@ucsd.edu).

Received 16 December 2015; accepted 8 March 2016; published online 11 April 2016; doi:10.1038/nn.4282

adult spinal cord using conditional knockout. Additionally, we demonstrate that a Ryk monoclonal antibody can be a therapeutic tool blocking Ryk function after lesion for improved functional recovery. A large proportion of patients have incomplete spinal cord injuries, providing a substrate for recovery. Our work illustrates that promoting circuit plasticity is a promising approach to restore function.

RESULTS

Ryk cKO enhances recovery of fine motor control after SCI

Mice underwent 2 weeks of training for the reaching and grasping task, followed by a C5 dorsal column spinal cord lesion: a partial spinal cord injury model leaving the dorsal gray matter, lateral white matter and the entire ventral spinal cord intact (Fig. 1a,d,e). Immediately after dorsal column lesion, forelimb reaching and grasping function is lost (Fig. 1f). With continued training, the success rate of sugar pellet retrieval recovers due to reconfiguration of neural circuits⁵. Studies have shown that the CST undergoes robust collateral sprouting after injury, and some of the new sprouts are thought to be responsible for new functional circuits^{10–13}. However, axon sprouting is inhibited by molecular cues that limit axon plasticity^{14,15}.

Members of the Wnt glycoprotein family are phylogenetically conserved axon guidance molecules that direct the growth along the rostrocaudal axis of both ascending sensory axons and descending CST axons during development^{6,16}. The repulsive Wnt receptor, Ryk, which mediates Wnt repulsion of the developing CST neurons, is either not expressed in the normal adult motor cortex and CST neurons or expressed at extremely low levels, below the detection limits of *in situ* hybridization or immunohistochemistry⁷. Spinal cord injury re-induces expression of Ryk mRNA and Ryk protein in the injured CST. By injecting function-blocking antibodies to Ryk and diffusible Wnt inhibitors, it was found that inhibiting Wnt–Ryk signaling enhanced the plasticity of both sensory and motor axons following injury^{7–9}. However, Ryk antibodies or Wnt inhibitors may exert the effects by impacting on the environment, such as the glial cells around the lesion, rather than CST axons *per se*.

To specifically test the role of Ryk in neurons, we created a Ryk conditional allele (cKO) and crossed these mice with Ai14 B6.Cg mice containing a *loxP*-flanked stop cassette preventing tdTomato expression, in order to specifically label recombinant corticospinal axons after viral transduction (Fig. 1b,c, Supplementary Fig. 1). We injected these Ryk cKO::tdTomato Ai14 mice with an adeno-associated virus (AAV) that expresses Cre recombinase under the control of the cytomegalovirus (CMV) promoter into the primary motor cortex and assessed the enhancement of corticospinal circuit remodeling (Fig. 1a). We injected AAV-Cre into adult motor cortex an average of 2.3 weeks before C5 dorsal column lesion in order to ensure sufficient time for Cre expression so that injury would not lead to Ryk expression. We found that Ryk deletion in the CST significantly

enhanced recovery of skilled forelimb function, as assessed by forelimb reaching and grasping, over a period of 12 weeks (repeated-measures ANOVA $P < 0.005$, Fig. 1f, Supplementary Fig. 2). Mice displayed the effects of Ryk deletion early on, with a trend toward better performance at early testing sessions. We observed this consistently; it may be a result of reduced retraction of axons and collaterals as previously demonstrated at 5 weeks post-injury in animals infused with Ryk antibodies⁷. Following Ryk conditional deletion, mice recovered to $81 \pm 7\%$ of peak pre-injury success rates, compared to only $60 \pm 5\%$ in control mice.

Ryk cKO enhances CST collateral sprouting after spinal cord injury

To begin to address the mechanisms underlying improved functional recovery in Ryk cKO mice, we analyzed CST collaterals and synapse density along collateral sprouts in the cervical spinal cord. We found that conditional Ryk deletion did not significantly reduce axonal die-back of the injured CST (one-tailed *t*-test $P = 0.12$) but did lead to significantly increased numbers of CST collaterals within the spinal gray matter, both rostral and caudal to the site of C5 injury, at 12 weeks post-injury (one-tailed *t*-test $P < 0.05$, Fig. 2). In addition to a greater number of axon collaterals, mice with Ryk conditionally deleted from cortical pyramidal neurons exhibited presynaptic vesicular glutamate transporter 1 (vGlut1)-labeled puncta on identified corticospinal axon collaterals at 600 μm rostral to the injury site, suggesting enhanced functional connectivity following Ryk conditional deletion (Fig. 3a–c).

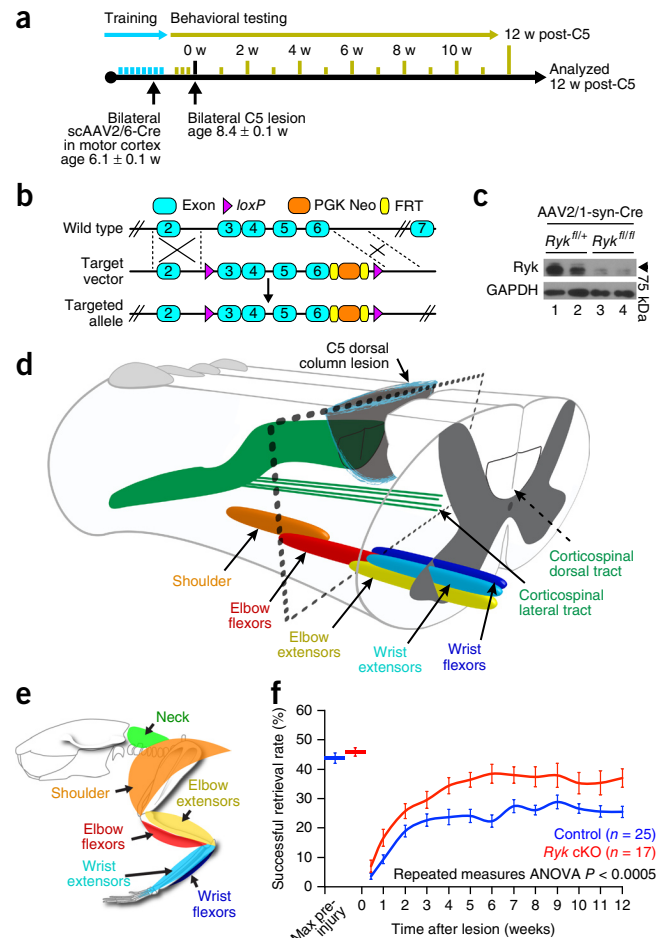
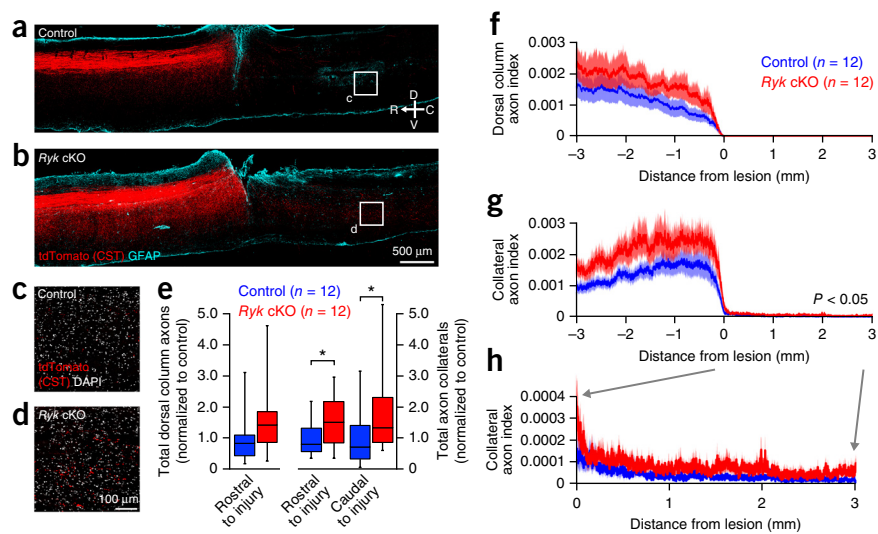


Figure 1 Ryk conditional deletion enhances motor function recovery from spinal cord injury. **(a)** Timeline outlining experimental details of the bilateral C5 dorsal column lesion (w, week). **(b,c)** Generation of Ryk conditional allele. **(b)** Exons 3–6 were flanked with *loxP* sites. **(c)** Western blot of postnatal day 7 motor cortex extract from mice injected at postnatal day 0 with AAV2/1 synapsin Cre. Full-length blot presented in Supplementary Figure 1. **(d,e)** Schematic showing the level of the C5 lesion in relation to motor neuron pools for distinct forelimb muscle groups (adapted from ref. 33 with permission). **(f)** Behavioral performance on skilled forelimb reach food-pellet retrieval task shows enhanced recovery after Ryk cKO in bilateral motor cortex ($n = 25$ mice (control), 17 mice (Ryk cKO), from 21 litters, repeated-measures ANOVA $P = 0.0003$, $F_{1,40} = 16.0102$). Data presented as mean \pm s.e.m.

Figure 2 *Ryk* conditional deletion enhances corticospinal axon sprouting after spinal cord injury. (a,b) Representative images of tdTomato-labeled CST axons from eight serial sagittal cryosections spaced 140 μ m apart superimposed over glial fibrillary acidic protein (GFAP) astroglial staining at the center of injury (1 experiment, $n = 12$ mice/group, from 11 litters; compass showing dorsal (D), ventral (V), rostral (R), and caudal (C)). *Ryk* cKO mice had greater levels of collateralization both rostral and caudal to the lesion than control mice (one-tailed t -test, $*P < 0.05$). (c,d) Higher magnification of single confocal planes from boxed regions (1.5 mm caudal to the lesion site) indicated in a and b, respectively. (e) Sum of tdTomato labeled axons (normalized to pyramidal labeling) over 3 mm rostral to lesion relative to control in the dorsal columns ($n = 12$ mice/group, one-tailed t -test $P = 0.12$, $t_{21} = 1.198$) and in the gray matter. *Ryk* cKO mice had greater levels of collateralization both rostral and caudal to the lesion than control mice ($n = 12$ mice/group, one-tailed t -test $*P < 0.05$: rostral $P = 0.0499$, $t_{19} = 1.730$, caudal $P = 0.0397$, $t_{19} = 1.855$). (f–h) Distribution of corticospinal axons (axon index is thresholded pixels every 0.411 μ m in 8 total sagittal spinal cord cryosections divided by thresholded pixels in transverse pyramids) within the dorsal columns (f) or spinal gray matter (g,h). (h) Magnified view of rostral collaterals from g. C5 injury site is at 0 μ m, rostral is represented with negative numbers, caudal with positive. Data in e presented as median with interquartile range; data in f–h presented as mean \pm s.e.m.



Most CST axons reside within the dorsal columns and are lesioned by the C5 dorsal column injury. A sparse, minor component of CST axons descend down the spinal cord within the lateral columns (lateral CST), which remained intact in our C5 lesion paradigm and may contribute to functional recovery⁵ (Fig. 1d). To test this, we first characterized the distribution of axon collaterals in the spinal cord both rostral and caudal to the C5 lesion. We observed an increase in axon collateral density in *Ryk* conditionally deleted mice throughout the gray matter, with the highest density more medial, in close proximity to the principal dorsal column corticospinal tract (Fig. 3a,d), suggesting that most of the increased branches may come from the dorsal column CST following *Ryk* deletion. No axons were present within the dorsal column CST caudal to C5 lesion in any of the mice studied.

To further assess the contribution of the dorsal column CST to behavioral recovery, we performed a second dorsal column lesion in

these animals 12 weeks after C5 injury at the C3 level, 1.15 \pm 0.07 mm rostral to the original C5 injury (Fig. 4a,b). The lateral CST is again spared in this lesion. We waited 1 week before behavioral testing to allow the mice to recover from the immediate hyporeflexic stage of spinal shock¹⁷. The secondary injury at C3 ablated the enhanced functional recovery we observed in the *Ryk* conditional deletion mice, leaving only the modest levels of partial recovery achieved by control mice (Fig. 4c). This suggests that the axon sprouts from the dorsal column CST are indeed responsible for the enhanced functional recovery in the *Ryk* conditional knockout. This also suggests that the spared lateral CST axons may provide only a minor contribution to a basal level functional recovery, independent of the dorsal column corticospinal tract. Quantification of axon distribution at 2 weeks after C3 lesion confirmed that the secondary C3 injury eliminated a majority of axon collaterals between

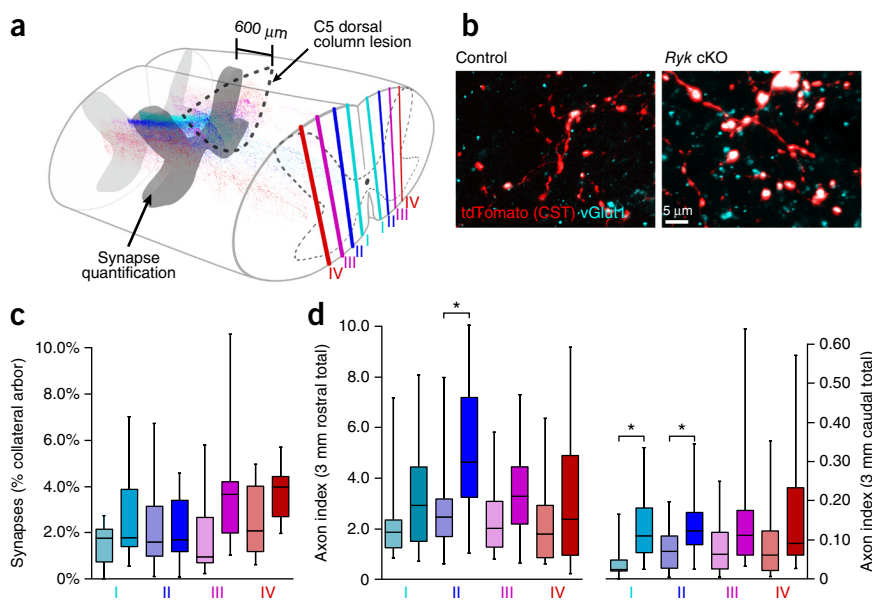


Figure 3 Changes in corticospinal connectivity after C5 dorsal column lesion. (a) Schematic showing the medio-lateral locations of cryosections for quantifications of synapse numbers and axon index in c and d. (b) Both control and *Ryk* conditional deletion mice showed pre-synaptic densities (vGlut1 colocalization with tdTomato-labeled corticospinal axons) at 600 μ m rostral to the C5 injury site (1 experiment, $n = 9$ mice/group). (c) Medio-lateral distribution of corticospinal innervation at 600 μ m rostral to C5 injury site. All data presented as median and inter-quartile range. For each color, lighter shade indicates control and darker shade indicates *Ryk* cKO ($n = 12$ mice/group). (d) Medio-lateral distribution of corticospinal axons shows the highest increase in collaterals proximal to the main dorsal corticospinal tract (regions I and II) after *Ryk* cKO ($n = 12$ mice/group, one-tailed t -test $*P < 0.05$: II rostral $P = 0.0225$, $t_{19} = 2.146$; II caudal $P = 0.0295$, $t_{21} = 1.996$; I caudal $P = 0.0059$, $t_{17} = 2.819$). Color code as in c.

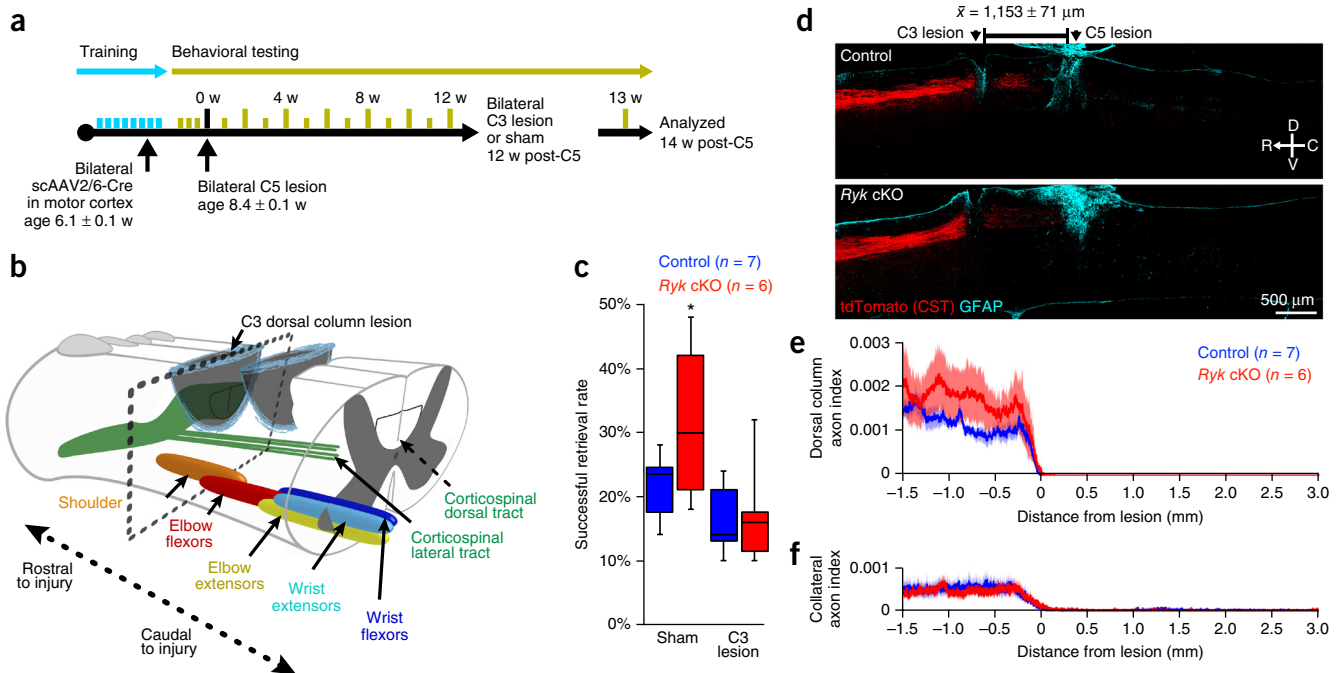


Figure 4 A second injury at C3 eliminates enhanced recovery. **(a)** Timeline outlining experimental details of secondary C3 lesion experiments following recovery from bilateral C5 dorsal column lesion. **(b)** Schematic of secondary C3 injury, above the level of increased presynaptic density shown in **Figure 3a–c**. **(c)** Behavioral performance on skilled forelimb reach food-pellet retrieval task shows elimination of enhanced recovery after *Ryk* cKO by second C3 dorsal column lesion (1 experiment, control (sham $n = 8$ mice, C3 $n = 7$), *Ryk* cKO (sham $n = 6$, C3 $n = 6$), mice from 14 litters, ANOVA $P = 0.0102$, $F_3 = 4.7432$, Bonferroni-corrected t -test $*P < 0.05$: *Ryk* cKO sham vs. control sham, $P = 0.0106$; *Ryk* cKO sham vs. *Ryk* cKO after C3 lesion, $P = 0.0092$). **(d–f)** Secondary C3 dorsal column lesion eliminated enhanced levels of collateralization in *Ryk* cKO mice. **(d)** Representative images of tdTomato-labeled CST axons from 8 serial sagittal cryosections spaced 140 μm apart superimposed over GFAP astroglial staining at the center of injury (1 experiment, 7 control, 6 *Ryk* cKO mice). **(e,f)** Distribution of corticospinal axons (axon index as described above) within the dorsal columns **(e)** or spinal gray matter **(f)**. C3 injury site is at 0 μm ; rostral is represented with negative numbers, caudal with positive. Data in **c** presented as median and interquartile range; data in **e,f** presented as mean \pm s.e.m.

the two injury sites, thereby disrupting the remodeled corticospinal circuit (**Fig. 4d–f**).

Monoclonal *Ryk* antibody promotes functional recovery

To test whether inhibition of the Wnt–*Ryk* signaling axis in the injured spinal cord after spinal cord injury is sufficient to increase CST remodeling and enhance behavioral recovery, we generated a new monoclonal *Ryk* antibody using half of the Wnt binding domain (amino acid range 90–183) as the antigen and infused into adult rats immediately following dorsal column lesion (**Fig. 5a,d**, **Supplementary Fig. 3**). We have previously generated function-blocking polyclonal antibodies using the same region⁷. Following a C5 dorsal column wire-knife lesion, *Ryk* antibody infusion via osmotic minipump for 4 weeks promoted recovery of skilled forelimb function in the forelimb reach task with all rats recovering to peak pre-injury levels, as compared to only half of rats infused with IgG control (**Fig. 5b**). *Ryk* antibodies did not enhance recovery in the grid-crossing locomotor task since rats exhibited similar levels of forelimb stepping impairment irrespective of treatment group (**Fig. 5c**). We labeled corticospinal axons by injecting biotinylated dextran amine (BDA) into the motor cortex. Consistent with the conditional *Ryk* deletion before injury, we found that the *Ryk* monoclonal antibody infusion at the time of injury resulted in an increase in corticospinal axon collaterals both rostral and caudal to the level of injury (one-tailed t -test $P < 0.05$, **Fig. 5e–i**, **Supplementary Fig. 4**). The extent of increase in collateral sprouts after *Ryk* antibody infusion in rats was similar to that observed in CST axons lacking *Ryk* expression in mice (**Figs. 2e** and **5i**). These results also suggest that *Ryk* signaling is a

feasible therapeutic target, since functional recovery can be promoted by blocking its function after spinal cord injury.

Cortical map reorganization during recovery

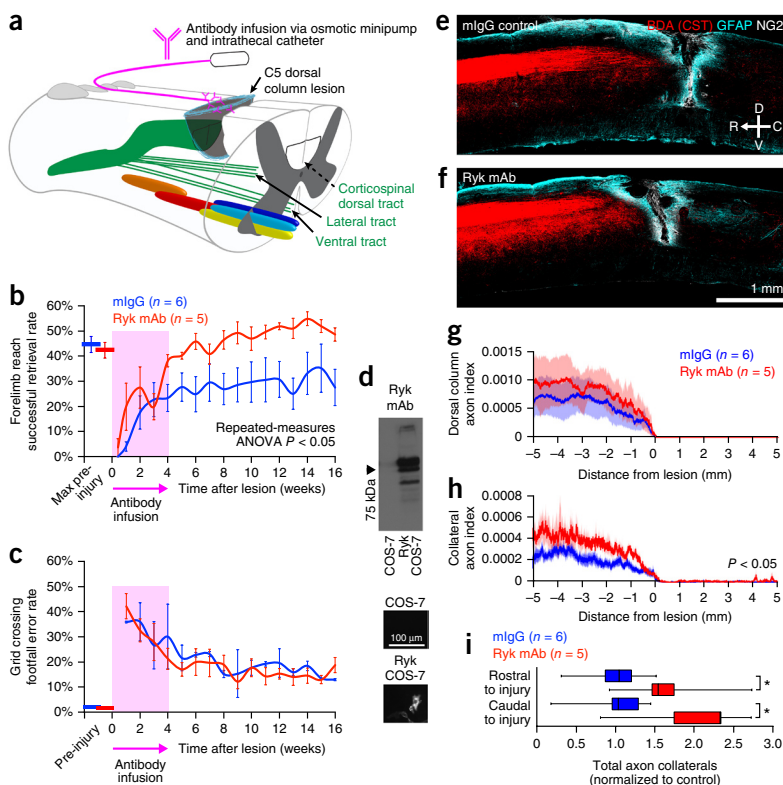
In order to address the circuit mechanisms with which the primary motor cortex regains control over the remodeled spinal cord, we used an optogenetic approach to monitor cortical output. Cortical motor maps have been studied using intracortical electrical stimulation in rodents and primates, as well as transcranial magnetic stimulation in humans^{18–21}. Recent advances in optogenetic tools allow for the stimulation of specific neural populations in a minimally invasive manner²². Specifically, the expression of the light-activated, non-selective cation channel channelrhodopsin-2 (*ChR2*) under the control of the *Thy1* promoter (*Thy1-ChR2*) allows for selective activation of layer V projection neurons within the motor cortex²². We performed unilateral craniotomies on *Thy1-ChR2* mice contralateral to the dominant forelimb in order to investigate motor map changes through repeated optogenetic mapping of evoked motor output after injury^{23,24} (**Supplementary Fig. 5**). Following craniotomy, we injected AAV-Cre unilaterally into the motor cortex contralateral to the dominant forelimb, as the contralateral cortex exhibits motor plasticity in response to forelimb training²⁵. We assessed motor map output by observing evoked, contralateral motor outputs in sedated mice and compared *Ryk* cKO with wild-type or heterozygote controls.

We observed massive remapping of cortical motor output immediately after spinal cord injury in the mouse (**Supplementary Fig. 6a,b**). Acutely (3 d) after C5 injury, the total area of motor representations

Figure 5 Monoclonal Ryk antibody infusion promotes functional recovery from spinal cord injury. (a) Schematic showing antibody infusion by intrathecal catheterization. (b) Behavioral performance on forelimb reach skilled food-pellet retrieval task shows enhanced recovery in rats infused with Ryk monoclonal antibody (mAb) for 28 d starting at time of injury ($n = 6$ rats (IgG control), 5 rats (Ryk mAb), repeated-measures ANOVA $P = 0.0354$, $F_{1,9} = 6.113$).

(c) Behavioral performance on skilled locomotor grid crossing task was not affected by Ryk mAb infusion. (d) Ryk mAb recognizes full-length Ryk protein expressed in transfected COS-7 cells by Western and immunocytochemistry. (e–h) BDA-labeled corticospinal axons in rats infused with Ryk mAb had greater levels of collateralization than control mouse-IgG-infused rats. (e, f) Images of BDA-labeled CST axons from six serial sagittal cryosections spaced 280 μm apart superimposed over GFAP astroglial and neural-glial antigen 2 (NG2) staining at the center of injury. (g, h) Distribution of corticospinal axons (axon index is thresholded pixels every 0.741 μm in 6 total sagittal spinal cord cryosections divided by thresholded pixels in transverse pyramids) within the dorsal columns (g) or spinal gray matter (h). C5 injury site is at 0 μm , rostral is represented with negative numbers, caudal with positive.

(i) Sum of normalized axon collaterals over 5 mm relative to control. Rats infused with Ryk mAb had greater levels of collateralization both rostral and caudal to the lesion than control mouse IgG infused rats ($n = 6$ rats (IgG control), 5 rats (Ryk mAb), one-tailed t -test $*P < 0.05$; rostral $P = 0.0446$, $t_6 = 2.000$; caudal $P = 0.0196$, $t_6 = 2.594$). Data in b, c, g, h presented as mean \pm s.e.m.; data in i presented as median and interquartile range.



for limb muscles at or below the level of the lesion was reduced or eliminated (Supplementary Fig. 6c). Conversely, motor maps expanded for muscle groups with motor neurons above the injury

site, most notably elbow flexion mediated by biceps brachii and brachialis (Figs. 6 and 7a, b, Supplementary Fig. 6c). Over the next 2 months following spinal cord lesion, cortical maps underwent gradual

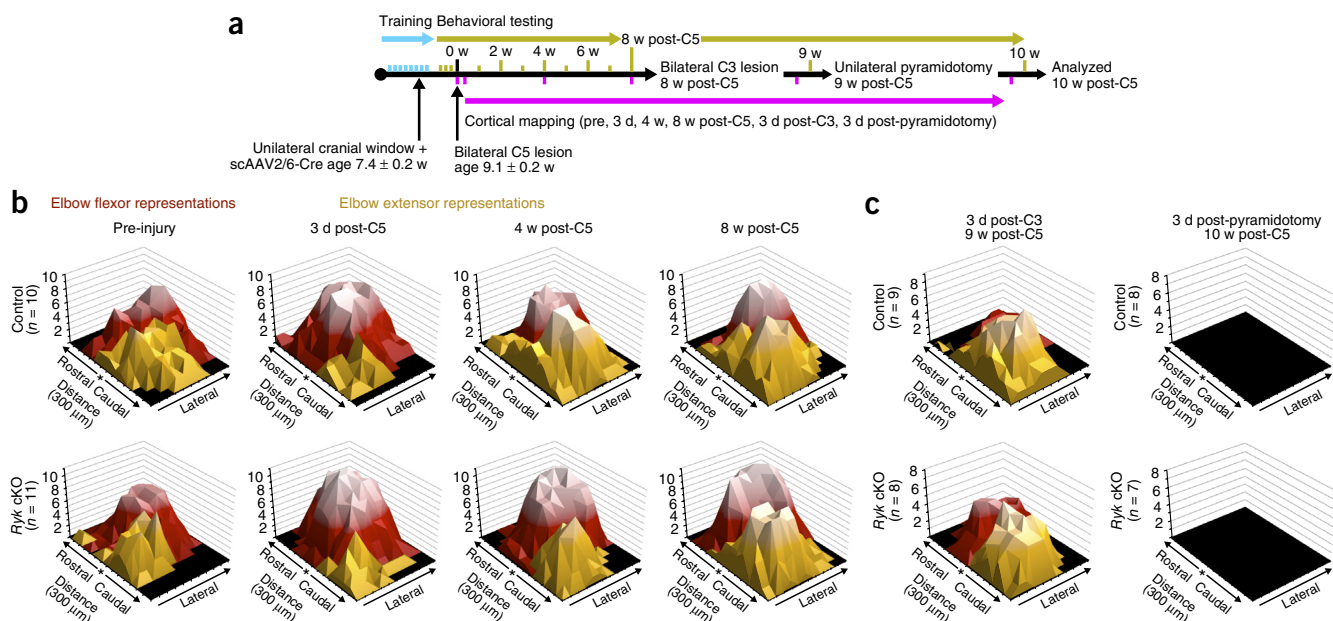


Figure 6 Cortical map reorganization during recovery from spinal cord injury. (a) Timeline outlining experimental details of optogenetic mapping with weekly behavioral testing following bilateral C5 dorsal column lesion. (b) Topographic representation of elbow flexor and extensor activation, relative to bregma (*), before and 3 d, 4 weeks and 8 weeks after C5 dorsal column lesion. Data presented as total number of mice responding with evoked movements at each location; lighter color indicates a larger number of mice are responsive at a given location. Each tic mark represents 300 μm . (c) Subsequent C3 dorsal column lesion disrupts remodeled circuitry, while subsequent pyramidotomy eliminates unilateral evoked motor output. Both were measured at 3 d after injury.

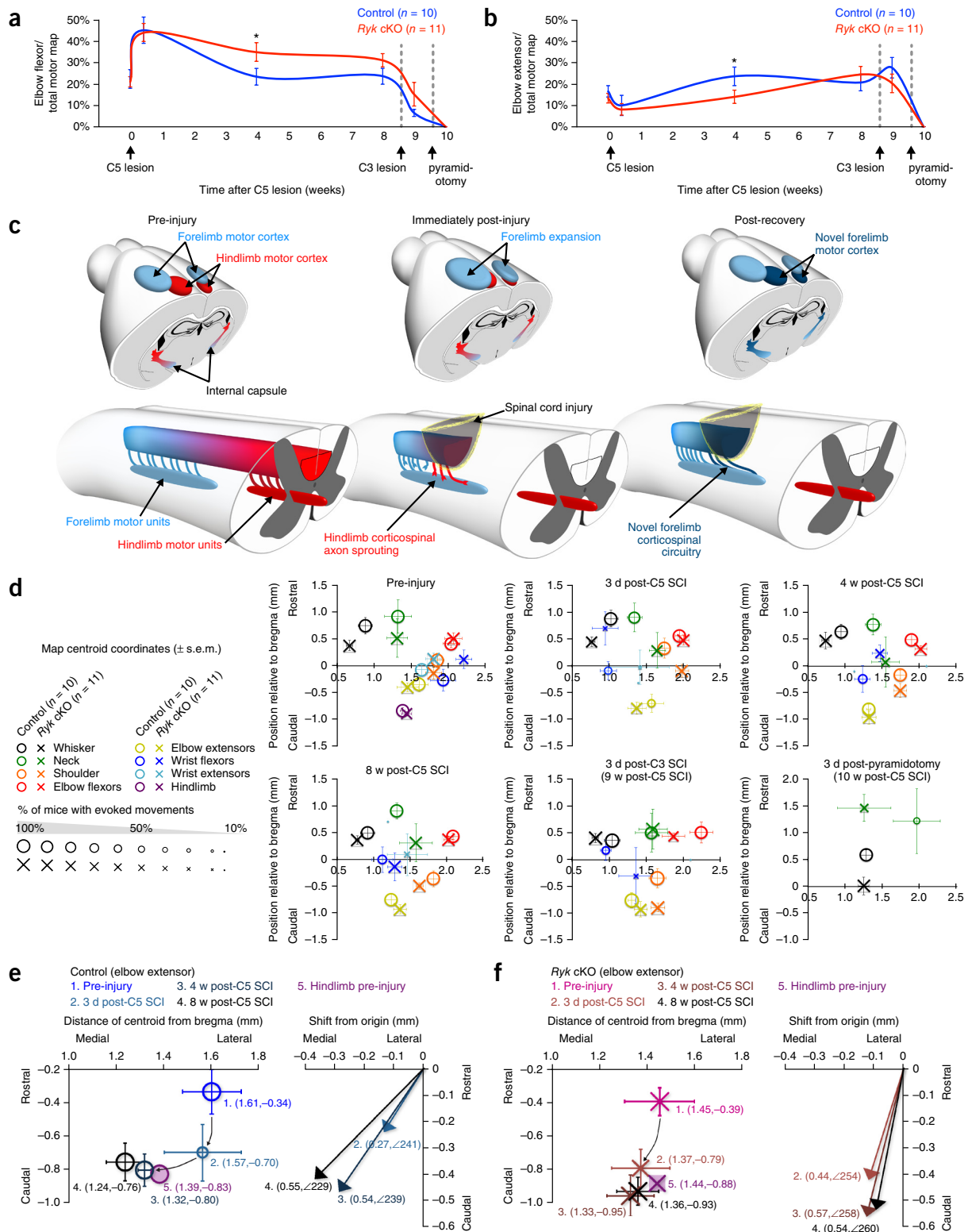
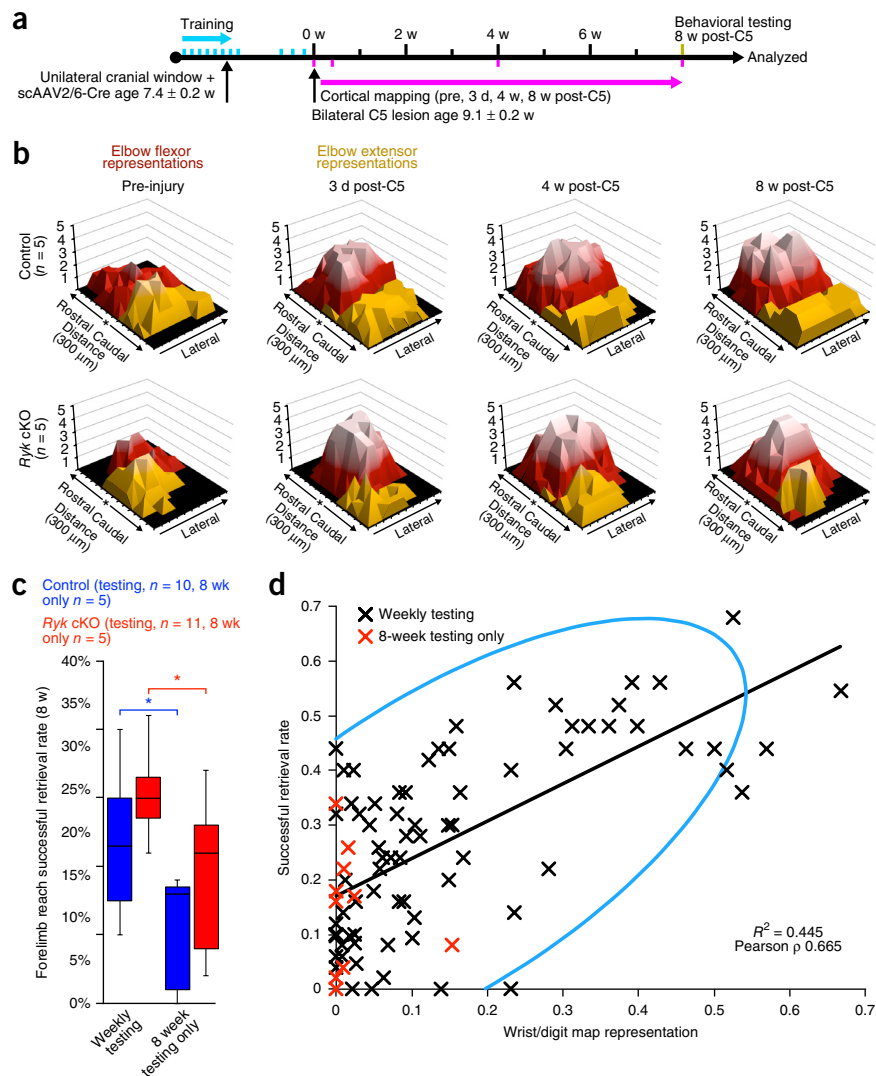


Figure 7 Forelimb motor map representations move into quiescent former hindlimb cortical areas. **(a,b)** Mice with *Ryk* cKO have a greater proportion of motor cortex devoted to elbow flexor activation at 4 weeks after C5 lesion **(a)** and, conversely, a smaller proportion devoted to extensor activation **(b)** ($n = 10$ (control) 11 (*Ryk* cKO) mice, one-tailed *t*-test $*P < 0.05$: elbow flexion $P = 0.0347$, $t_{19} = 1.925$, elbow extension $P = 0.0460$, $t_{16} = -1.791$, data presented as mean \pm s.e.m.). **(c)** Model for recruitment of ectopic cortical motor regions mediated by axon plasticity. After dorsal column injury, the immediate expansion of forelimb regions above the level of injury is likely mediated by lateral connectivity within the motor cortex. Increased axonal plasticity and connectivity after *Ryk* cKO likely drives the formation of novel, ectopic areas of forelimb motor cortex. **(d)** Cortical map reorganization from spinal cord injury in mice that received weekly training demonstrates how map centroids shift after injury. Size of the marker is proportional to the percentage of mice with evoked motor movements of a given muscle group. **(e,f)** Elbow extensor motor maps shift caudally and medially toward cortex originally occupied by hindlimb representations.

Figure 8 Cortical map reorganization and functional recovery from spinal cord injury are dependent upon rehabilitative training.

(a) Timeline outlining experimental details of optogenetic mapping with only terminal behavioral testing at 8 weeks post-injury. (b) Topographic representation of elbow flexor and extensor activation, relative to bregma (*), before and 3 d, 4 weeks, and 8 weeks after C5 dorsal column lesion in the absence of weekly behavioral testing. (c) At 8 weeks after C5 dorsal column lesion, mice with weekly behavioral testing, both *Ryk* cKO and controls, performed better than those tested only at 8 weeks ($n = 10$ (control weekly testing), 11 (*Ryk* cKO weekly testing), 5 (control 8-week testing only), 5 *Ryk* cKO (8-week testing only) mice, ANOVA $P = 0.0037$, $F_3 = 5.7157$, Bonferroni-corrected t -test $*P < 0.05$: (i) *Ryk* cKO weekly vs. only 8-week testing $P = 0.0277$, (ii) control weekly vs. only 8-week testing $P = 0.0346$; data presented as median and interquartile range). (d) In animals with weekly behavioral testing (black Xs), there was a strong correlation of wrist movement and skilled forelimb reach performance, regardless of injury or genotype ($n = 84$ measurements (4 time points, 21 mice), bivariate Pearson correlation P , $P < 0.0001$, $\rho = 0.665$). Blue arc is density ellipse ($\alpha = 0.95$). Mice with no weekly behavioral testing are indicated in red.

changes with continued forelimb reaching and grasping training (Supplementary Fig. 6). Behavioral recovery after C5 spinal cord injury plateaued between 4 and 8 weeks post-injury (Fig. 1f, Supplementary Fig. 7), with a median time to reach 90% of peak post-injury performance of 6 weeks in control mice and 5 weeks in *Ryk* conditional deletion mice. Therefore, we examined cortical motor maps before and after peak recovery, at 4 weeks and 8 weeks post-injury, respectively. At 4 weeks post-injury, we observed significant differences in the proportion of motor cortex allocated to forelimb extensor (biceps) or forelimb flexor (triceps) activation, with *Ryk*-deleted mice exhibiting larger flexor motor maps at the expense of extensor maps ($P < 0.05$, one-tailed t -test, Fig. 7b,c, Supplementary Fig. 6a,b). Expansion of elbow extensor areas at 4 weeks into regions originally occupied by the flexor was inversely correlated with behavioral recovery ($n = 21$ mice: 10 (control), 11 (*Ryk* cKO), Spearman's $\rho = -0.5766$, $P = 0.0062$). By 8 weeks post-injury, *Ryk*-deleted mice exhibited a pattern of extensor and flexor motor maps similar to that of controls; however, the total area occupied by all elbow movements (flexor and extensor) was significantly larger in *Ryk*-deleted mice (one-tailed t -test, $P = 0.0480$, $t_{14} = 1.79$). Additionally, at 8 weeks post-injury, wrist flexor representations returned to (or exceeded) maximal pre-injury size in 64% of *Ryk*-deleted mice compared to 10% of control mice (Wilcoxon rank sum $P = 0.0136$, $\chi^2 = 6.086$, Supplementary Fig. 6c). Recovery of wrist flexor control correlated with improvement of forelimb reach performance at 8 weeks post-injury (Spearman's $\rho = 0.4555$, $P = 0.0380$). Over the course of the experiment, there was a strong correlation of wrist movement and skilled forelimb reach performance, regardless of injury or genotype (Pearson's $\rho = 0.665$, $P < 0.0001$, Fig. 8d).



In order to further characterize the remapped cortical output, mice were subjected to a second dorsal column lesion at C3, rostral to the level of extensor motor units, at 8 weeks after C5 injury (Fig. 4b). We found that the C3 injury significantly reduced flexor motor maps in all mice but, surprisingly, had little effect on the recovered extensor motor maps, suggesting the flexor control is routed from connections rostral to C3 or from the lateral corticospinal tract (Fig. 6d, Supplementary Fig. 6a,b). Importantly, a subsequent unilateral pyramidotomy abolished unilateral forelimb responses to cortical stimulation and also the ability of mice to perform the forelimb reach task (Fig. 6c, Supplementary Figs. 6a,b and 7). Although plasticity of other supraspinal pathways, such as the rubrospinal tract or reticulospinal tract, may also contribute to functional recovery, the effects of unilateral pyramidotomy suggest that a direct connection between the primary motor cortex with the cervical spinal cord is essential for the recovered skilled forelimb movement (Supplementary Fig. 6a,b).

Cortical re-organization requires rehabilitative training

The repeated testing of skilled forelimb reach over the course of the experiment essentially constitutes a rehabilitative training paradigm that can promote motor recovery from spinal cord injury and cortical reorganization^{26,27}. In order to determine if the induced axonal

plasticity mediated by Ryk deletion alone was sufficient to promote functional recovery, we tested the recovery of skilled forelimb reach at 8 weeks after C5 injury in another cohort of mice that did not undergo weekly behavioral testing after injury (Fig. 8a). Mice that did not undergo weekly behavioral testing displayed only limited skilled forelimb recovery with performance similar to that of mice tested at 1 week after injury (Figs. 8c and 1f). In the absence of weekly testing, refinement of cortical motor maps was also impaired, irrespective of Ryk conditional deletion (Fig. 8b, Supplementary Fig. 8).

DISCUSSION

In order to understand how neural circuits reorganize to regain function after injury, we performed functional, anatomical and behavioral analyses. We demonstrate here that the motor cortex remaps such that the cortical areas no longer used for the hindlimb are recruited to control the forelimb to achieve functional recovery after a C5 dorsal column lesion and this reorganization requires continued training. We also showed that removing Ryk, a receptor for the Wnt family of axon guidance cues, results in greater CST axon plasticity and cortical circuit remodeling in conjunction with rehabilitative training, leading to maximal functional restoration. The more gradual and persistent changes in cortical control maps observed in injured Ryk cKO mice are likely due to the enhanced changes in connectivity within the spinal cord and cortical circuits that occur in the absence of Wnt–Ryk signaling. We found previously that Wnt–Ryk signaling controls topographic map formation in the developing visual system²⁸. Here we reveal a novel function of Wnt–Ryk signaling in controlling motor cortex remapping after spinal cord injury in adulthood.

Previous studies demonstrated that somatosensory cortical maps expand into affected neighboring regions after spinal cord injury^{10,11}. We characterized the motor output map after spinal cord injury and show here that forelimb motor maps spread into adjacent regions affected by injury. We observed an expansion of flexor control area caudally and medially toward cortical regions originally responsible for hindlimb movements (Fig. 7d,e, Supplementary Fig. 6a,b). These changes are likely stereotypical, because wrist flexor representations exhibited a medial shift as they recovered, similar to observed shifts of digit representations in primates²⁹ (Fig. 7d, Supplementary Fig. 6a,b).

Alterations of motor output maps have been noted in spinal cord injury patients for many years, but the neural circuit mechanisms remain unknown. In rats, naive transected hindlimb-projecting corticospinal neurons sprout into the cervical spinal cord as early as 1 week after spinal cord injury¹¹. However, it is unlikely that early expansion of motor maps above the level of the injury, which we observed only 3 d later in mice, was due to sprouting and establishment of new connectivity patterns; rather, it is likely due to a loss of inhibition within the cortex²¹. By 4 weeks after spinal cord injury, cortical maps likely reflect the output to the remodeled corticospinal circuitry in the cervical spinal cord. We observed that the greater CST axon collateral numbers induced following Ryk deletion lead to a slight increase in connections with motor units distal to the injury site but a greater increase with those rostral to the injury (Figs. 2h and 3b). Therefore, the changes in connectivity above the level of injury could be the main source for the changes of cortical maps (Fig. 7f). For example, the initial expansion of the biceps control areas at 4 weeks post-injury, and subsequent reduction at 8 weeks, may result from an initial sprouting of all CST collaterals that project to the forelimb motor units in the cervical spinal cord, followed by a subsequent pruning through Hebbian competition. The recruitment of the hindlimb cortical areas for triceps control may result from *de novo* connections to the forelimb motor units of the cervical spinal cord

from corticospinal neurons that originally projected to the hindlimb. These sprouts may either directly contact motor units or form relays using propriospinal neurons. Conditional deletion of Ryk in corticospinal neurons enhances collateral sprouts and thus may recruit more spinal cord circuitry, a process that likely underlies greater recovery of skilled forelimb function. The results of our antibody infusion experiments in the spinal cord suggest that circuit remodeling in the cervical spinal cord is sufficient to promote functional recovery. However, it is plausible that connectivity changes within the primary motor cortex also contribute to the remodeling of the entire circuit.

Other descending pathways are also involved in fine motor control and can partially compensate for the loss of CST input on a skilled forelimb reach task³⁰. Additionally, animals with incomplete lesion of the pyramids have been shown to exhibit similar success rates of skilled forelimb reach to intact control animals through compensatory forelimb movements, indicating that a small proportion of spared CST is capable of restoring full, if altered, function on the skilled forelimb reach task³¹. In 59% of our Ryk cKO mice and 100% of Ryk monoclonal antibody-infused animals, we achieved recovery of skilled forelimb reach to levels at or above peak pre-injury levels. In our dorsal column lesion model, this full recovery clearly requires the novel CST connections rostral to the lesion, as a second C3 lesion abolishes the enhanced recovery. While the CST is not the sole component mediating control of skilled forelimb reach, it is required for the recovered function, as pyramidotomy in our mouse model completely abolished the reaching and grasping behavior. These results suggest that restoring at least some CST function is a critical component in optimal recovery of motor control after injury, as compensatory plasticity of other tracts drives limited recovery in rodents, which are less dependent upon the CST for motor control than primates.

In this study, we also demonstrate that a Ryk monoclonal antibody can be a therapeutic tool, as blocking Ryk function after lesion leads to improved functional recovery. We show here that maximal recovery of the forelimb can be achieved by combining targeted plasticity for the forelimb function (continued reaching and grasping training) and molecular manipulation. Therefore, we anticipate that combining targeted plasticity of other functions with molecular manipulation may allow recovery of other motor or sensory functions. A large proportion of patients have incomplete spinal cord injuries, providing a substrate for recovery³². Our work illustrates that promoting circuit plasticity is a promising approach to restore maximal function following incomplete spinal cord injury.

METHODS

Methods and any associated references are available in the [online version of the paper](#).

Note: Any Supplementary Information and Source Data files are available in the online version of the paper.

ACKNOWLEDGMENTS

We would like to thank Z. He, B. Zheng, F. Wang, L. Wang and the members of the Zou lab for critical reading of the manuscript, as well as comments and suggestions. This work was supported by grants to Y.Z. (RO1 NS047484, R21 NS081738, Wings for Life Foundation, and International Foundation for Research in Paraplegia).

AUTHOR CONTRIBUTIONS

Y.Z. and E.R.H. designed the experiments. E.R.H., N.I., T.Y., C.-C.L., A.H., K.T., A.R., A.T., M.P. and E.J. performed all the experiments under the supervision of Y.Z. Y.Z. designed the antigen for the Ryk monoclonal antibody. C.-C.L. and A.R. prepared the antigen. S.-H.W. generated the hybridomas using the antigen under the supervision of A.K. A.T. and E.R.H. screened for the hybridoma and tested the function of the Ryk monoclonal antibody *in vitro* and *in vivo*.

COMPETING FINANCIAL INTERESTS

The authors declare no competing financial interests.

Reprints and permissions information is available online at <http://www.nature.com/reprints/index.html>.

- Lemon, R.N. & Griffiths, J. Comparing the function of the corticospinal system in different species: organizational differences for motor specialization? *Muscle Nerve* **32**, 261–279 (2005).
- Whishaw, I.Q., Pellis, S.M., Gorny, B.P. & Pellis, V.C. The impairments in reaching and the movements of compensation in rats with motor cortex lesions: an endpoint, video recording, and movement notation analysis. *Behav. Brain Res.* **42**, 77–91 (1991).
- Metz, G.A.S., Dietz, V., Schwab, M.E. & van de Meent, H. The effects of unilateral pyramidal tract section on hindlimb motor performance in the rat. *Behav. Brain Res.* **96**, 37–46 (1998).
- Schmidlin, E., Wannier, T., Bloch, J. & Rouiller, E.M. Progressive plastic changes in the hand representation of the primary motor cortex parallel incomplete recovery from a unilateral section of the corticospinal tract at cervical level in monkeys. *Brain Res.* **1017**, 172–183 (2004).
- Weidner, N., Ner, A., Salimi, N. & Tuszynski, M.H. Spontaneous corticospinal axonal plasticity and functional recovery after adult central nervous system injury. *Proc. Natl. Acad. Sci. USA* **98**, 3513–3518 (2001).
- Liu, Y. *et al.* Ryk-mediated Wnt repulsion regulates posterior-directed growth of corticospinal tract. *Nat. Neurosci.* **8**, 1151–1159 (2005).
- Liu, Y. *et al.* Repulsive Wnt signaling inhibits axon regeneration after CNS injury. *J. Neurosci.* **28**, 8376–8382 (2008).
- Hollis, E.R. II *et al.* Remodeling of spared proprioceptive circuit involving a small number of neurons supports functional recovery. *Nat. Commun.* **6**, 6079 (2015).
- Hollis, E.R. II & Zou, Y. Reinduced Wnt signaling limits regenerative potential of sensory axons in the spinal cord following conditioning lesion. *Proc. Natl. Acad. Sci. USA* **109**, 14663–14668 (2012).
- Bareyre, F.M. *et al.* The injured spinal cord spontaneously forms a new intraspinal circuit in adult rats. *Nat. Neurosci.* **7**, 269–277 (2004).
- Ghosh, A. *et al.* Rewiring of hindlimb corticospinal neurons after spinal cord injury. *Nat. Neurosci.* **13**, 97–104 (2010).
- Takeoka, A., Vollenweider, I., Courtine, G. & Arber, S. Muscle spindle feedback directs locomotor recovery and circuit reorganization after spinal cord injury. *Cell* **159**, 1626–1639 (2014).
- van den Brand, R. *et al.* Restoring voluntary control of locomotion after paralyzing spinal cord injury. *Science* **336**, 1182–1185 (2012).
- Giger, R.J., Hollis, E.R. II & Tuszynski, M.H. Guidance molecules in axon regeneration. *Cold Spring Harb. Perspect. Biol.* **2**, a001867 (2010).
- Hollis, E.R. II. Axon guidance molecules and neural circuit remodeling after spinal cord injury. *Neurotherapeutics* doi:10.1007/s13311-015-0416-0 (2015).
- Lyuksyutova, A.I. *et al.* Anterior-posterior guidance of commissural axons by Wnt-frizzled signaling. *Science* **302**, 1984–1988 (2003).
- Ditunno, J.F., Little, J.W., Tessler, A. & Burns, A.S. Spinal shock revisited: a four-phase model. *Spinal Cord* **42**, 383–395 (2004).
- Leyton, A.S.F. & Sherrington, C.S. Observations on the excitable cortex of the chimpanzee, orang-utan, and gorilla. *Exp. Physiol.* **11**, 135–222 (1917).
- Streletz, L.J. *et al.* Transcranial magnetic stimulation: cortical motor maps in acute spinal cord injury. *Brain Topogr.* **7**, 245–250 (1995).
- Topka, H., Cohen, L.G., Cole, R.A. & Hallett, M. Reorganization of corticospinal pathways following spinal cord injury. *Neurology* **41**, 1276–1283 (1991).
- Jacobs, K.M. & Donoghue, J.P. Reshaping the cortical motor map by unmasking latent intracortical connections. *Science* **251**, 944–947 (1991).
- Arenkiel, B.R. *et al.* In vivo light-induced activation of neural circuitry in transgenic mice expressing channelrhodopsin-2. *Neuron* **54**, 205–218 (2007).
- Ayling, O.G.S., Harrison, T.C., Boyd, J.D., Goroshkov, A. & Murphy, T.H. Automated light-based mapping of motor cortex by photoactivation of channelrhodopsin-2 transgenic mice. *Nat. Methods* **6**, 219–224 (2009).
- Hira, R. *et al.* Transcranial optogenetic stimulation for functional mapping of the motor cortex. *J. Neurosci. Methods* **179**, 258–263 (2009).
- Kleim, J.A., Barbay, S. & Nudo, R.J. Functional reorganization of the rat motor cortex following motor skill learning. *J. Neurophysiol.* **80**, 3321–3325 (1998).
- Girgis, J. *et al.* Reaching training in rats with spinal cord injury promotes plasticity and task specific recovery. *Brain* **130**, 2993–3003 (2007).
- Fouad, K. & Tetzlaff, W. Rehabilitative training and plasticity following spinal cord injury. *Exp. Neurol.* **235**, 91–99 (2012).
- Schmitt, A.M. *et al.* Wnt-Ryk signaling mediates medial-lateral retinotectal topographic mapping. *Nature* **439**, 31–37 (2006).
- Nishimura, Y. *et al.* Time-dependent central compensatory mechanisms of finger dexterity after spinal cord injury. *Science* **318**, 1150–1155 (2007).
- García-Álías, G., Truong, K., Shah, P.K., Roy, R.R. & Edgerton, V.R. Plasticity of subcortical pathways promote recovery of skilled hand function in rats after corticospinal and rubrospinal tract injuries. *Exp. Neurol.* **266**, 112–119 (2015).
- Piecharka, D.M., Kleim, J.A. & Whishaw, I.Q. Limits on recovery in the corticospinal tract of the rat: partial lesions impair skilled reaching and the topographic representation of the forelimb in motor cortex. *Brain Res. Bull.* **66**, 203–211 (2005).
- Morawietz, C. & Moffat, F. Effects of locomotor training after incomplete spinal cord injury: a systematic review. *Arch. Phys. Med. Rehabil.* **94**, 2297–2308 (2013).
- McKenna, J.E., Prusky, G.T. & Whishaw, I.Q. Cervical motoneuron topography reflects the proximodistal organization of muscles and movements of the rat forelimb: a retrograde carbocyanine dye analysis. *J. Comp. Neurol.* **419**, 286–296 (2000).

ONLINE METHODS

All animal work in this research was approved by the University of California, San Diego (UCSD) Institutional Animal Care and Use Committee. Animals were housed on a 12 h light/dark cycle and behavioral analyses were done at consistent morning hours during the light cycle. Both mice and rats were group housed, except for mice with cranial windows which were singly housed after window implantation. Group sample sizes were chosen based upon previous studies and power analysis (25% effect size, $\alpha = 0.05$, $\beta = 0.2$, power of 80%). One mouse was excluded from the study due to evidence of incomplete C5 lesion with labeled corticospinal axons present at and below the level of the injury and one mouse was excluded as it did not attempt to perform the behavioral task after injury. All procedures and methods (surgical procedures, behavioral assays, tissue processing, immunostaining, image analysis, COS-7 transfection, and cortical mapping) were performed by investigators blinded to genotype or treatment group.

Generation of transgenic mice. The target vector containing *loxP*-flanked exons 3–6 as well as the PKG-neo selection cassette was transfected into ES cells at the UCSD Transgenic Core facility. Cells were screened by Southern blot and PCR for integration of the targeting vector. Chimeric mice were generated at the UCSD Transgenic Core facility. *Ryk* cKO mice were crossed with Ai14 B6.Cg mice containing a *loxP*-flanked stop cassette preventing tdTomato expression (The Jackson Laboratory, Bar Harbor, ME, RRID:IMSR_JAX:007914) and backcrossed into C57BL/6J for six generations. For cortical mapping experiments, *Ryk* cKO::tdTomato Ai14 mice were crossed with mice expressing channelrhodopsin (Chr2) behind the Thy1 promoter (B6.Cg-Tg(Thy1-COP4/EYFP)18Gfng/J) (The Jackson Laboratory).

Surgical procedures. *Cortical AAV injection.* Adult female C57BL/6J mice (6.1 ± 0.1 weeks old) were deeply anaesthetized with isoflurane until unresponsive to toe and tail pinch and the area over the skull was shaved and cleaned with povidone-iodine before incision. The skull was thinned bilaterally over the motor cortex and self-complementary AAV2/6 Cre-HA (Salk Institute for Biological Studies Gene Transfer, Targeting and Therapeutics Core, La Jolla, CA) (1.49×10^{11} genome copies per ml) was injected into ten sites per hemisphere (250 nl per site) with a 36 ga NanoFil needle (World Precision Instruments Inc., Sarasota, FL).

Cranial window. Adult female C57BL/6J mice (7.4 ± 0.2 weeks old) were deeply anaesthetized with isoflurane. The skin over the skull was removed, the skull surrounding the motor cortex contralateral to the dominant forelimb was thinned, the skull over the motor cortex was removed, and self-complementary AAV2/6 Cre-HA was injected to ten sites as above. The exposed cortex was covered with a 5 mm #1 round glass coverslip (Warner Instruments, Hamden, CT) secured with VetBond (3M, St. Paul, MN). The exposed skull was covered with dental grip cement (Dentsply, York, PA).

C5 and C3 dorsal column lesion (mice). Mice were deeply anaesthetized with isoflurane, spinal level C5 (or C3) was exposed by laminectomy and the dorsal columns were lesioned at a depth of 1 mm with Vannas spring scissors (Fine Science Tools, Foster City, CA). The dorsal musculature was sutured with 4-0 silk sutures and the skin was closed with wound clips. Mice were randomly selected for C3 lesion or C3 sham (laminectomy only) groups.

Pyramidotomy. Mice were deeply anesthetized with ketamine (120 mg per kg body weight) and xylazine (12 mg per kg), an incision was made and the ventral musculature was pushed aside to expose the pyramids. The dura was opened and the pyramid ipsilateral to the craniotomy was lesioned by 15° microscalpel (Electron Microscopy Sciences, Hatfield, PA) as previously described³⁴.

C5 dorsal column lesion (rats). Adult female Fischer 344 rats (120–135 g) were deeply anaesthetized with 2 ml/kg of ketamine cocktail (25 mg per ml ketamine, 1.3 mg per ml xylazine and 0.25 mg per ml acepromazine). Spinal level C5 was exposed by laminectomy, the dura was punctured over the dorsal horn, and the dorsal columns were lesioned with two passes of a Scouten wire-knife (David Kopf Instruments, Tujunga, CA). The dorsal musculature was sutured with 4-0 silk sutures and the skin was closed with wound clips. Polyethylene intrathecal catheters (Durect Corp., Cupertino, CA) were pre-filled with either mouse IgG or Ryk monoclonal IgG (clone 25.5.5 generated against the ectodomain of Ryk, amino acid range 90–183, by Johns Hopkins Monoclonal Antibody Core, Baltimore, MD) (1 mg per ml) in artificial cerebrospinal fluid, threaded through the magna cisterna to the cervical spinal cord, secured with 4-0 silk sutures,

and attached to model 2004 osmotic minipumps (Durect Corp.) filled with 200 μ l mouse IgG or Ryk IgG. Rats were randomly selected for mouse IgG or Ryk monoclonal IgG treatment. Osmotic minipumps were removed after 28 days. At 16 weeks after C5 spinal cord injury, rats were injected bilaterally with 10% wt per vol 10,000 MW biotinylated dextran amine (BDA) in sterile phosphate buffered saline at 20 sites per hemisphere (250 nl per site); animals were killed 2 weeks later.

Cortical mapping. Mice were lightly anaesthetized with a ketamine (100 mg per kg)–xylazine (10 mg per kg) mixture, still responsive to toe and tail pinch, and maintained during the course of stimulation with ketamine–xylazine mixture. Mice were fixed in a stereotaxic frame (David Kopf Instruments) and a fiber optic cable and cannulae (200 μ m diameter) affixed to the stereotaxic arm were used to stimulate motor cortex locations relative to bregma that were unobstructed by skull or dental cement (maximum of 165 sites). Stimulation was 3 pulses of 470 nm light, 250 ms duration at 1 Hz from a single channel LED driver (Thorlabs, Newton, NJ). The intensity of stimulation was increased from 50 mA up to 1,000 mA until movement was detected in 3 consecutive pulses. Sites with no evoked movements at 1,000 mA were scored as unresponsive. Only contralateral forelimb movements were scored; occasional, weaker, ipsilateral movements were observed as previously described in rats³⁵.

Ryk knockout in postnatal day 0 pups. Pups were injected with 0.5 μ l of AAV2/1-synapsin-Cre (Penn Vector Core, Philadelphia, PA) (1.99×10^{13} genome copies per ml) into two sites in the motor cortex unilaterally with a 36 ga NanoFil needle (World Precision Instruments Inc.). Mice were killed 7 days later and the motor cortex was isolated and homogenized in lysis buffer (20 mM Tris HCl, pH 7.5, 150 mM NaCl, 1 mM EDTA, 1 mM EGTA, 10 mM NaF, 10 mM β -glycerophosphate, 1 mM Na_2VO_4 , 0.5% wt per vol sodium dodecyl sulfate, 1% vol per vol TritonX-100, and cOmplete protease inhibitor cocktail (Roche, Indianapolis, IN). Protein was analyzed by Western blot (40 μ g per well). Antibodies used for Western mouse: anti-Ryk (20 μ g per ml) (Johns Hopkins Monoclonal Antibody Core), GAPDH (1:1,000) (EMD Millipore, Billerica, MA, catalog #MAB374, RRID:AB_2107445).

Tissue processing. Animals were deeply anaesthetized with ketamine cocktail, transcardially perfused with ice-cold PBS followed by 4% wt per vol paraformaldehyde in phosphate buffered saline (PBS), and brains and spinal columns were post-fixed overnight at 4 °C in 4% wt per vol paraformaldehyde. Tissue was cryoprotected in 30% wt per vol sucrose in PBS. Mouse spinal cords and brainstems, and rat brainstems were sectioned on a cryostat (Leica, Buffalo Grove, IL) at 20 μ m (sagittal spinal cords, transverse brainstems) and mounted directly on Superfrost Plus slides (Fisher Scientific, Pittsburgh, PA). Rat spinal cords were sectioned sagittally at 40 μ m thick and collected as free-floating sections. Sections were washed three times with PBS, blocked for one hour in PBS with 0.25% triton-X100 (PBST) and 5% donkey serum, then incubated overnight at 4 °C with primary antibodies in PBST plus 5% donkey serum. The next day, sections were washed three times, incubated with Alexa Fluor conjugated secondary antibodies (Life Technologies, Grand Island, NY; Jackson ImmunoResearch, West Grove, PA) for 2.5 h at room temperature, counterstained with DAPI (1 μ g per ml) (Sigma-Aldrich, St. Louis, MO) and washed three final times in PBS. Antibodies used for fluorescent immunohistochemistry were: rabbit anti-dsRed (1:1,000) (Clontech Laboratories Inc., Mountain View, CA, catalog #632496, RRID:AB_10013483), monoclonal G-A-5 anti-GFAP (1:200) (Sigma-Aldrich, catalog #G3893, RRID:AB_2314539), guinea pig anti-vGlut1 (1:1,000) (EMD Millipore, catalog #AB5905, RRID:AB_2301751), and rabbit anti-GFAP (1:750) (Dako, Carpinteria, CA, catalog #Z0334, RRID:AB_10013382).

COS-7 cell transfection. COS-7 cells were transfected with pcDNA4-Ryk using FuGene6 (Roche) to express full length Ryk. Cells were either fixed for 30 min with ice-cold 4% wt per vol paraformaldehyde in PBS for immunocytochemistry, or lysed with lysis buffer for Western blot.

Image acquisition and analysis. Images were acquired on an inverted Zeiss LSM510 confocal microscope with LSM acquisition software (Carl Zeiss Microscopy, LLC, Thornwood, NY). Image density quantification was done on thresholded images using ImageJ (NIH, Bethesda, MD). An investigator blinded to the experimental group performed all analyses. Axon index is the total thresholded pixels every 0.411 μ m in eight total serial sagittal spinal cord

cryosections spaced 140 μm apart for mice, or 0.741 μm in six total serial sagittal spinal cord cryosections spaced 280 μm apart for rats, divided by thresholded pixels in transverse sections of the pyramid at the level of the obex. Lesion volume was calculated using the Cavalieri estimator tool in StereoInvestigator (MBF Bioscience, Williston, VT) on every seventh 40 μm sagittal section. For tdTomato and vGlut1 colocalization, all axons within the gray matter were quantified over a region 210 μm wide at a distance of 600 μm rostral to the C5 lesion in the eight total serial sagittal cryosections used for tdTomato quantification. The location of 600 μm was chosen it is where as we observed the highest density of axon collaterals in this region in both groups of animals (**Fig. 1g**) and because it is located between the original C5 and secondary C3 lesions.

Behavioral testing. All animals were trained on the skilled forelimb reach task over a period of two weeks before bilateral spinal cord injury. Animals were food restricted during training and then for 24 h before weekly training after injury. Animals reached through a vertical slot in the front of an acrylic chamber and over a small gap to retrieve a reward pellet. Mice performed 25 reaches per session for 20 mg sucrose reward tablets (TestDiet, St. Louis, MO). Rats performed 50 reaches per session for 45 mg sugar pellets (Bio-Serv, Flemington, NJ). Successful retrieval rate was calculated as the number of pellets that were retrieved and eaten divided by the number contacted by the forepaw. Animals were trained in the forelimb reach task twice weekly by two independent investigators blind to genotype or experimental treatment; the two independent scores were averaged. Mice in the group without weekly training during recovery were only tested twice, at 8 weeks after injury. In addition to forelimb reach, rats were tested once weekly

on a grid crossing task, where forelimb footfalls were calculated as a percentage of total forelimb steps in three passages over a 60 inch span of 1 inch equidistant wire grid.

Statistics. Statistical tests indicated in main text were performed using JMP 9 software (SAS Institute, Cary, NC). We have previously demonstrated that inhibition of repulsive Wnt signaling results in sprouting and plasticity of descending corticospinal and ascending dorsal column sensory axons after spinal cord injury^{7–9}. In addressing our hypothesis that *Ryk* cKO or *Ryk* monoclonal antibody enhanced axon sprouting, we tested the increases by one-tailed *t*-test (**Figs. 2e, 3d and 5i** and **Supplementary Fig. 3**). In order to test longitudinal behavioral studies with multiple, equally spaced measurements, we used repeated-measures ANOVA (**Figs. 1f and 5b** and **Supplementary Fig. 6**). In testing multiple groups with continuous, parametric data, we used ANOVA with post-hoc Bonferroni correction on appropriate post-hoc comparisons (**Figs. 4c and 8c**). Bivariate correlation was performed to determine the relationship between forelimb function and cortical maps (**Fig. 8d**). Continuous data was tested with parametric tests and data was assumed to be normally distributed, but this was not formally tested.

A **Supplementary Methods Checklist** is available.

34. Lee, J.K. *et al.* Assessing spinal axon regeneration and sprouting in Nogo-, MAG-, and OMgp-deficient mice. *Neuron* **66**, 663–670 (2010).
35. Liang, F., Rouiller, E.M. & Wiesendanger, M. Modulation of sustained electromyographic activity by single intracortical microstimuli: comparison of two forelimb motor cortical areas of the rat. *Somatosens. Mot. Res.* **10**, 51–61 (1993).